

Ag and IL-2 immune complexes efficiently expand Ag-specific Treg cells that migrate in response to chemokines and reduce localized immune responses

Ryoko Hamano<sup>1</sup>, Tomohisa Baba<sup>2</sup>, Soichiro Sasaki<sup>2</sup>, Utano Tomaru<sup>3</sup>, Akihiro Ishizu<sup>4</sup>, Mitsuhiro Kawano<sup>1</sup>, Masakazu Yamagishi<sup>5</sup> and Naofumi Mukaida<sup>2</sup>

<sup>1</sup>Division of Rheumatology, Department of Internal Medicine, Kanazawa University Hospital, Kanazawa, Ishikawa, Japan

<sup>2</sup>Division of Molecular Bioregulation, Cancer Research Institute, Kanazawa University, Kanazawa, Ishikawa, Japan

<sup>3</sup>Department of Pathology/Pathophysiology, Graduate School of Medicine, Hokkaido University, Sapporo, Hokkaido, Japan

<sup>4</sup>Faculty of Health Science, Hokkaido University, Sapporo, Hokkaido, Japan

<sup>5</sup>Division of Cardiology, Department of Internal Medicine, Kanazawa University Hospital, Kanazawa, Ishikawa, Japan

Key words: CCR2, thymus, Treg cells

Corresponding author: Tomohisa Baba

Division of Molecular Bioregulation, Cancer Research Institute, Kanazawa University, Kakuma-machi, Kanazawa, Japan, 920-1192

sergenti@staff.kanazawa-u.ac.jp

Fax: +81 76 234 4520, Phone: +81 76 264 6736

Abbreviations used in this article: cDC, conventional DC; CFSE, carboxyfluorescein diacetate succinimidyl ester; dLN, draining LN; DTH, delayed-type hypersensitivity; FCM, flow cytometry; IL-2 ICs, IL-2-anti-IL-2 Ab immune complex; iTreg, induced Treg; nTreg, naturally occurring Treg; Teff, effector T cell; tRANTES, truncated RANTES

## Summary

An intravenous administration of a high-dose Ag can induce immune tolerance and suppress the immune response, but the mechanism remains unclear. We recently proved that a combined intravenous administration of OVA and IL-2-anti-IL-2 Ab immune complexes (IL-2 ICs) efficiently expands OVA-specific Treg cells in the thymus and induces their migration into peripheral blood, by using OVA-specific T-cell receptor Tg-expressing DO11.10 mice. Here, we demonstrate that the expanded OVA-specific Treg cells rapidly move into the air pouch after OVA injection in DO11.10 mice. The migration was inhibited by blocking the axis of a chemokine receptor, CCR2. Moreover, prior treatment with OVA and IL-2 ICs enhanced OVA-specific Treg-cell migration and inhibited OVA-induced delayed-type hypersensitivity (DTH) reactions in the skin of BM chimeric mice with 15 % of T cells expressing OVA-specific T-cell receptor. Blocking the CCR2 axis reversed this suppression of DTH in these mice. Furthermore, prior treatment with OVA and IL-2 ICs effectively reduced DTH reactions even in WT mice possessing only a very small population of OVA-specific T cells. Thus, the treatment with Ag and IL-2 ICs can efficiently expand Ag-specific Treg cells with the capacity to migrate and reduce localized immune responses.

## Introduction

Recognition of a foreign substance initiates adaptive immunity, thereby generating Ag-specific T cells and Abs. The immune system can recognize autologous molecules as well as exogenous ones, but the immune reaction against an autologous Ag can cause a deleterious condition, the autoimmune response. The thymus has a crucial role in the prevention of autoimmune responses by educating a T-cell precursor, the thymocyte, to become unresponsive to autologous Ags. This process, called intrathymic education, consists of two processes, negative selection and differentiation of naturally occurring Treg (nTreg) cells. Negative selection eliminates thymocytes, which can recognize autologous Ags with high affinity, while nTreg can inhibit the effector T (Teff) cell response to autologous Ags in an Ag-specific manner.

The mode of immune response can differ depending on the dose of Ag, the route of administration, and the presence of adjuvant. Subcutaneous or dermal injection of a protein emulsified in adjuvant can activate T cells [1], whereas oral exposure to an Ag can induce tolerance [2]. Moreover, an intravenous injection of a high-dose Ag can induce Ag-specific immune tolerance [3-5] and can prevent autoimmune diseases in mice such as type 1 diabetes mellitus [6] or EAE [4]. Although intrathymic education is generally vital to induce immune tolerance, the role of the thymus in immune tolerance induced by an intravenous injection of a high-dose Ag needs further clarification.

IL-2 is one of the most important cytokines for Treg-cell development and survival [7]. Moreover, Webster et. al. [8] observed that in vivo administration of IL-2 immune complexes (ICs) can induce a marked increase in Treg cells in many organs, including the liver and gut as well as the spleen and LNs, with a modest increase in Treg cells in the thymus. Furthermore, pre-treatment with IL-2 ICs rendered mice resistant to induction of EAE and induced tolerance to fully MHC-incompatible pancreatic transplants [8].

We previously demonstrated that thymic CD11c<sup>+</sup>CD11b<sup>+</sup>CD8α<sup>-</sup>Sirpα<sup>+</sup> conventional DCs (cDCs) are preferentially localized in an interlobular vascular-rich region and that they can selectively capture blood-circulating Ag and induce Ag-specific Treg-cell generation, thereby inducing immune tolerance in the thymus [9, 10]. We therefore postulated that the combined intravenous injection of an Ag and IL-2 ICs could expand Ag-specific Treg cells with a capacity to migrate to the Ag-containing site, thereby reducing Ag-specific immune responses. In order to prove this assumption, we examined the effects of combined intravenous injection of OVA and IL-2 ICs on an OVA-induced DTH reaction in the skin. We provide here definitive evidence indicating that the treatment generated Ag-specific Treg cells in thymus which could migrate preferentially to the DTH site in a CCR2-dependent manner, thereby dampening the DTH reaction.

## Results

### **Ag-specific Treg cells preferentially migrate to an Ag-containing site.**

We first examined whether Ag-specific Treg cells could migrate to the Ag injection site. In order to address this point, we repeated intravenous OVA injection to DO11.10 mice twice before OVA administration into air pouch (Figure 1A). This resulted in the rapid appearance of KJ1-26<sup>high</sup>Foxp3<sup>-</sup> Teff cells in the air pouch within 12 h after OVA administration (Figure 1B). Subsequently, KJ1-26<sup>high</sup>Foxp3<sup>+</sup> Treg cells accumulated in the air pouch more than 24 h after OVA injection, comprising more than 20% of the total KJ1-26<sup>high</sup> cells (Figure 1B). The administration of BSA into the air pouch failed to induce KJ1-26<sup>high</sup>Foxp3<sup>+</sup> Treg-cell accumulation (Figure 1C), suggesting that a localized Ag at the induced inflammatory site can attract Ag-specific Treg cells. In order to test this assumption, we collected lymphocytes from DO11.10 mice either immunized twice with OVA or non-immunized. These cells were labeled with carboxyfluorescein diacetate succinimidyl ester (CFSE) and administered to WT mice (Supporting Information Figure 1A). Subsequent administration of OVA into air pouch of such recipient mice induced the accumulation of CFSE-labeled immunized KJ1-26<sup>high</sup>Foxp3<sup>+</sup> Treg cells but not non-immunized cells in the air pouch (Figure 1D). Furthermore, the in vivo primed Treg cells, in which CFSE signal was diluted by the cell division, mainly accumulated in the air pouch (Figure 1D). Consequently, Ag-specific Treg cells can migrate to the site containing the Ag.

### **Intravenously administered Ag induces intrathymic Treg cells and their migration into the periphery**

We previously demonstrated that an intravenous injection of an Ag can induce differentiation of Ag-specific Treg cells in the thymus [10]. Untreated thymus contained a small number of both KJ1-26<sup>low</sup>Foxp3<sup>+</sup> and KJ1-26<sup>high</sup>Foxp3<sup>+</sup> cells (Supporting Information Figure 2). Following intravenous OVA injection,

KJ1-26<sup>high</sup>Foxp3<sup>+</sup> but not KJ1-26<sup>high</sup>Foxp3<sup>-</sup> thymocytes increased (Figure 2A, Supporting Information Figure 2, and 3). However, the KJ1-26<sup>high</sup>Foxp3<sup>+</sup> thymocyte number decreased at 5 days after OVA injection (Figure 2A). Concomitantly, KJ1-26<sup>high</sup>Foxp3<sup>+</sup> Treg cells appeared in peripheral blood 5 days after OVA injection (Figure 2B). The increase in KJ1-26<sup>high</sup>Foxp3<sup>+</sup> Treg cells in peripheral blood was reduced by removal of the thymus but not spleen (Figure 2C). Moreover, intravenous OVA injection increased Helios<sup>+</sup>Foxp3<sup>+</sup> Treg cells in the thymus, and to a lower extent, in the spleen (Figure 2D). Concomitantly, most Foxp3<sup>+</sup> cells in peripheral blood expressed Helios (Figure 2E). Finally, we obtained lymphocytes from DO11.10 mice, either immunized with OVA or non-immunized, and transferred them into the air pouch-bearing WT mice (Supporting Information Figure 1B). WT mice, which received non-immunized DO11.10 lymphocytes, were subsequently immunized with OVA to induce Treg cells mainly in the periphery. OVA injection into the air pouch led to a higher proportion of Foxp3<sup>+</sup> Treg cells among KJ1-26<sup>high</sup> cells at the air pouch, in the mice receiving the immunized lymphocytes than in the mice receiving unimmunized lymphocytes and subsequent intravenous OVA injection (Figure 2F). Thus, Ag-specific Treg cells, which were generated in the thymus, could migrate into the antigen site more efficiently than peripherally-induced Treg cells.

### **Ag-specific Treg cells migrate to the air pouch in a CCR2-dependent manner**

The selective migration of Ag-specific Treg cells prompted us to investigate the contribution of chemokines, which can exhibit chemotactic activities on a selected set of leukocytes with their receptors [11-13]. Flow cytometry (FCM) analysis demonstrated an enhanced expression of several chemokine receptors including CCR2, CCR4, CCR5, and CXCR4 on Ag-specific Treg cells infiltrating in Ag-injected air pouch, compared with Teff cells (Figure 3A). Of particular interest is that most Ag-specific Treg cells in the OVA-injected air pouch expressed CCR2, and that the expression level was higher than that in the draining LN (dLN). These observations

suggested the involvement of the ligands for these receptors in the migration of Ag-specific Foxp3<sup>+</sup> Treg cells into the air pouch. The administration of OVA into the air pouch consistently induced increases in the contents of CCL2, the ligand for CCR2, CCL17 and CCL22, the ligands for CCR4, and CCL5 (RANTES), the ligand for CCR5 (Supporting Information Figure 4), but not CXCL12, the ligand for CXCR4 (data not shown). In order to prove the roles of these chemokines, we blocked the axes of these chemokines. Consistent with the previous report [14, 15], anti-CCL17 and anti-CCL22 neutralizing Abs reduced the numbers of KJ1-26<sup>high</sup> Treg cells migrating into the OVA-injected air pouch with no effect on the proportion of KJ1-26<sup>high</sup> Treg cells in the draining lymph node (Supporting Information Figure 5). Accumulating evidence identifies truncated RANTES (tRANTES) as a potent antagonistic protein against CCR5 [16]. Moreover, in vivo transfection of tRANTES expression vector (Supporting Information Figure 6) can sustain serum tRANTES levels sufficient to block CCR5-mediated signals (our unpublished data). However, in vivo transfection of tRANTES-expressing vector failed to cause any significant changes in the number and proportion of KJ1-26<sup>high</sup> Treg cells, when compared with control vector (Supporting Information Figure 7). On the contrary, genetic ablation of CCR2 reduced the number and proportion of KJ1-26<sup>high</sup> Treg cells in the OVA-injected air pouch, but increased that of the dLN (Figure 3B). Because CCR2 is well-known as an essential factor for the monocyte and macrophage chemotaxis, it is possible that the reduced Treg-cell infiltration in CCR2<sup>-/-</sup> mice may be indirectly due to the less monocyte migration and reduction of infiltration. To exclude this possibility, lymphocytes from DO11.10 or DO11.10/CCR2<sup>-/-</sup> mice were transferred to WT mice bearing air pouch. OVA injection to the air pouch failed to attract the KJ1-26<sup>high</sup> Treg cells derived from DO11.10/CCR2<sup>-/-</sup> mice (Figure 3C). This proved that CCR2 expression on Treg cells is necessary for their migration to Ags. Thus, the expression of CCR2 can contribute to the preferential Ag-specific Treg-cell migration into the Ag-injected site.

### **Induced Ag-specific Treg cells migrate into DTH site and suppress an excessive reaction**

We next examined the function of intravenously administered Ag-induced Treg cells in more pathologically relevant condition. In order to examine the immune suppressive activities of these Ag-specific Treg cells in the experimental DTH model, we first injected OVA into the footpad of DO11.10 mice after subcutaneous immunization with OVA emulsified in CFA (Figure 4A). However, the intractable and marked DTH response ensued due to a massive infiltration of KJ1-26<sup>high</sup> Teff cells into the injected footpad (our unpublished data). In order to circumvent the intractable DTH, we prepared BM chimeric mice using WT and DO11.10 mice to obtain mice with about 10 to 15 % of T cells expressing DO11.10 clonotypic TCR (Supporting Information Figure 8). The resultant BM chimeric mice still exhibited a considerable DTH reaction as evidenced by an abundant leukocyte infiltration and an enhanced paw thickness (Figure 4B and 4C). Because the intravenous administration of OVA induced KJ1-26<sup>high</sup> Treg cell expansion (Figure 2A and 2B), IL-2 ICs was additionally administered in combination with the intravenous OVA injection (Figure 4A). Consistent with the previous report [8], IL-2 ICs alone induced the expansion of polyclonal V $\alpha$ 2<sup>+</sup> Treg cells, but not KJ1-26<sup>high</sup> Treg cells in peripheral blood, whereas the combined treatment with OVA and IL-2 ICs succeeded in expansion of KJ1-26<sup>high</sup> CD25<sup>+</sup>Foxp3<sup>+</sup> Treg cells as well as polyclonal Treg cells (Figure 4D and Supporting Information Figure 9). The combined treatment with OVA and IL-2 ICs, but not that with OVA or IL-2 ICs alone diminished the DTH reaction as evidenced by decreased leukocyte infiltration and reduced paw thickness (Figure 4B and 4C). Likewise, the combined treatment with OVA and IL-2 ICs, but not that with OVA or IL-2 ICs alone increased the proportion of Foxp3<sup>+</sup> cells in the inflammatory site (Figure 4E). Thus, in collaboration with IL-2 ICs, a prior intravenous injection of an Ag can expand Ag-specific Treg cells in the thymus and can induce their migration to the inflammatory sites to suppress local inflammation.

### **Reversion of Ag-IL-2 ICs-mediated suppression of DTH reaction by blocking CCR2**

We next examined whether Ag-specific Treg cells migrated into the Ag injection site to dampen DTH response in a CCR2-dependent manner, as observed on the air pouch model. Histological examination demonstrated that leukocytes infiltrated to the Ag-injected site to similar extents irrespective of the absence or the presence of *CCR2* gene (Figure 5A). However, Ag-IL-2 ICs suppressed leukocyte infiltration and paw thickness only in the presence of *CCR2* gene (Figure 5A and 5B). Similarly, Treg-cell infiltration was enhanced by Ag-IL-2 ICs treatment only in the presence of *CCR2* gene (Figure 5C). Likewise, neutralization of CCR4 ligands did abrogate the effects of Ag-IL-2 ICs treatment on DTH (Supporting Information Figure 10). Thus, Ag-specific Treg cells can utilize CCR2 and/or CCR4 to migrate into the Ag-localized site, thereby suppressing immune-mediated DTH reaction.

### **Successful immune control by combined treatment of IL-2 ICs and Ag in DTH**

Finally, we examined whether the combined treatment with an Ag and IL-2 ICs can dampen DTH reaction even in WT mice, which do not possess monoclonal or oligoclonal T cells. When OVA-immunized WT mice were challenged with a subcutaneous OVA injection, the mice exhibited DTH reaction as evidenced by subcutaneous leukocyte infiltration and enhanced paw thickness (Figure 6A and 6B), although the magnitude of the reaction was weaker than that of BM chimeric mice (compare between Figures 4C and 6A). The prior combined intravenous administration with OVA and IL-2 ICs, but not that with IL-2 ICs or OVA alone, markedly reduced leukocyte infiltration and paw thickness (Figure 6A and 6B). Thus, the combined intravenous injection of an Ag and IL-2 ICs can reduce local immune response probably by inducing intrathymic differentiation of Ag-specific Treg cells and their migration into the site of the immune response under the control of chemokine

receptors such as CCR2 and CCR4.

## Discussion

The administration of a high-dose Ag can induce immune tolerance by utilizing several mechanisms including depletion of Teff cells [4], induction of T-cell apoptosis in peripheral blood and thymus [5], suppression of Ig production [17], and expansion of Treg cells [18]. Here, we determined that an intravenous injection of a high-dose of Ag could efficiently expand Ag-specific Treg cells in a thymus-dependent manner and that the expansion could be further augmented by the additional administration of IL-2 ICs. Moreover, the expanded Ag-specific Treg cells preferentially migrated to the local injection site of Ag in a CCR2-dependent manner to prevent immune response-mediated DTH reactions.

We previously demonstrated that thymic  $CD11c^+CD11b^+CD8^-Sirp\alpha^+$  cDCs are principally located in interlobular vascular-rich region of the thymic cortex and capture Ags from bloodstream [9] to induce Ag-specific Treg-cell generation [10]. Also under the present conditions, we observed that Ag-specific Treg cells appeared in the circulation after their transient intrathymic expansion. Evidence is accumulating to indicate that Treg cells can be generated in the spleen and LNs as well as the thymus. However, the removal of thymus but not spleen markedly reduced the increase in Ag-specific Treg-cell numbers in peripheral blood. Helios, a member of Ikaros transcription factor family, was once reported to be a marker of thymus-derived Treg cells. Intravenous Ag injection induced Helios expression on Ag-specific Treg cells in the thymus but not spleen. Thereafter, Ag-specific Treg cells in circulation started to express Helios. Several lines of evidence questioned the validity of Helios as a specific marker of thymus-derived Treg cells [19, 20]. However, intravenous Ag injection efficiently increased the Ag-specific Treg cells, which were generated in the thymus and to a lesser extent, ones converted in the periphery in the Ag containing site. Thus, it is probable that an intravenous Ag injection could induce Treg-cell generation in the thymus, although Treg-cell conversion from other T-cell populations in the periphery

can also contribute to a certain extent.

Treg cells can be classified into two populations with distinct roles in immune tolerance, nTreg and induced Treg (iTreg) cells [21]. nTreg cells are generated in the thymus and can regulate mainly Th1 mediated-immune responses. On the contrary, iTreg cells are generated in the periphery outside the thymus and can control Th2 mediated-response in mucosal tolerance [22]. We demonstrated that an intravenous Ag injection can induce Ag-specific Treg cells in the thymus. Thus, the intrathymically generated Treg cells can suppress DTH reaction, a typical Th1-mediated immune response upon reaching local Ag injection site. Several immunosuppressive maneuvers were developed by using iTreg cells, which were either expanded *ex vivo* [23] or differentiated *in vitro* [24]. On the contrary, we provided the first definitive evidence to indicate the immunosuppressive potential of intrathymic differentiated Ag-specific Treg cells, which are expanded independently of AIRE [25].

Treg cells can be an attractive target cell type for immune regulation. Webster et. al. demonstrated that the administration of IL-2 ICs selectively expanded Treg cells, and prevented the development of EAE and induced tolerance to MHC-incompatible pancreatic transplants [8]. We observed that treatment with IL-2 ICs alone expanded polyclonal Treg cells. However, the expansion of polyclonal Treg cells can cause generalized Ag-non-specific immune suppression [26-29]. Thus, the expansion of Ag-specific Treg cells is preferable to polyclonally expanded Treg cells to avoid generalized immune suppression. We showed that intravenous treatment with both an Ag and IL-2 ICs efficiently expanded Ag-specific Treg cells and subsequently suppressed DTH, whereas IL-2 ICs treatment alone could neither expand Ag-specific Treg cells nor suppress DTH. Thus, Ag-specific Treg cells can suppress specific immune responses such as DTH more efficiently than polyclonal Treg cells.

Currently used immune-suppressive agents can inhibit immune reaction broadly and in an Ag-nonspecific manner. Thus, the use of Ag-specific Treg cells can be more effective and less harmful due to their selectivity. Moreover, the selectivity can be

further augmented by Ag-specific activation of Treg cells to exert their Ag-specific suppressive function *in vivo* [18]. Furthermore, once activated with an Ag, Ag-specific Treg cells can suppress additional immune reactions against other unrelated Ags in the organ exhibiting the specific Ag, resulting in organ-specific immune suppression against a broad range of Ags [30, 31]. We demonstrate that Ag-IL-2 ICs treatment can efficiently expand and activate Ag-specific Treg cells with the capacity to migrate to the organ containing a specific Ag. Thus, the present approach may be effective for organ-specific immune diseases, if pathogenic Ags or organ-specific Ags are definitively identified as in the case of contact dermatitis and GVHD.

It is of interest that the expanded Ag-specific Treg cells preferentially migrated to the Ag injection site in the peripheral tissue, both in air pouch model and DTH reaction. Treg cells can migrate into various sites such as the tumor tissues, infected site and transplanted organs [15, 32-34], to suppress immune response to the tumor, infected tissues, or transplanted organs [27, 35]. Leukocyte migration is controlled by several factors and among them, chemokines have a crucial role. Leukocytes can migrate in response to the interaction between chemokine(s) expressed in the local site and the chemokine receptor(s) expressed by leukocytes [36-38]. Several lines of evidence indicate that Treg migration into the peripheral tissue is regulated by CD103, CCR2, CCR4 and CCR5 expression [15, 16, 34, 39, 40]. In particular, it is broadly known that CCR4 signaling plays an important role in Treg cells migration [15]. We demonstrated that most Ag-specific Treg cells expressed CCR2 as well as CCR4 and CCR5, and that Ag-injected air pouch contained abundant CCL2, the ligand for CCR2. These results suggest that CCR2 also have crucial roles in Treg cells migration. This notion is further supported by our present observation that blocking CCR2-mediated signaling reduced Ag-specific Treg cells migration into the Ag site. Moreover, blocking the receptors reversed Ag-IL-2 ICs-mediated suppression of DTH reactions. CCR2-mediated signals apparently have essential roles in Ag-specific Treg-cell migration into the Ag containing site in addition to CCR4-mediated signals. CCR2

signal is known to have a main role in migration of macrophage and dendritic cells to initiate inflammation. But, on the other hand, CCR2 could also contribute to Ag-specific Treg-cell migration to suppress immune reaction. Thus, CCR2-mediated signals can supplement the use of Ag-specific Treg cells to control DTH-related immune responses.

## Materials and Methods

### Mice

Female Balb/c mice were obtained from Charles River Japan (Yokohama, Japan) and designated as WT mice. DO11.10 mice expressing a Tg TCR that recognizes the OVA323–339 peptide in the context of I-A<sup>d</sup> were maintained as heterozygotes. DO11.10/CCR2<sup>-/-</sup> mice were generated by mating DO11.10 and CCR2-deficient mice as previously described [9]. All mice were maintained in the animal facility of the Kanazawa University under specific pathogen-free conditions. All animal experiments were approved and performed according to the Guideline for the Care and Use of Laboratory Animals of Kanazawa University

### Reagents and Abs

Rat anti-mouse DO11.10 clonotypic TCR (KJ1-26), Foxp3 (MF23) and IL-2 (JES6-1A12) Abs were obtained from BD Bioscience (San Jose, CA). Rat anti-mouse CD4 (RM5-5) and Foxp3 (FJK-16s) Abs were obtained from eBioscience (San Diego, CA). Rat anti-mouse CD25 (PC61) and CD184/CXCR4 (TG12/CXCR4) Abs, and hamster anti-mouse CD194/CCR4 (2G12), Helios (22F6), and CD195/CCR5 (HMCCR5) Abs were obtained from BioLegend (San Diego, CA). Recombinant mouse IL-2, and rat anti-mouse CCL17/TARC (110904), CCL22/MDC (158132), and CD192/CCR2 (475301) Abs were obtained from R&D systems (Minneapolis, MN). OVA and BSA were obtained from Sigma Aldrich (St. Louis, MO).

### Air pouch model (Figure 1A)

Subcutaneous air pouches were prepared as described with some modifications [41]. Briefly, 5 ml of air was subcutaneously injected to dorsal surface of WT or DO11.10 mice. 2 mg of OVA dissolved in 200  $\mu$ L of PBS was injected intravenously twice, one and two days after the air injection. 3 ml of air was additionally injected into the air pouch on Day 3. On Day 4, 100  $\mu$ g of OVA in 1 ml of PBS was injected into the air

pouch. At the indicated time points after the last OVA injection into the air pouch, the cells in the air pouch were recovered by washing the air pouch with 1 ml of cold PBS. The obtained fluid samples were centrifuged to obtain the supernatants and the cell suspensions. The supernatants were used for the determination of chemokines by ELISA while the cell suspensions were used for cell surface marker analysis by FCM after the determination of the cell number. In some experiments, lymphocytes were collected from LNs of DO11.10 or DO11.10/CCR2<sup>-/-</sup> mice, which were untreated or intravenously administered with OVA as described above. The obtained cells were stained with 2  $\mu$ M of CFSE (Life Technologies Corporation, Carlsbad, CA), and were transferred to WT mice (Supporting Information Figure 1A and B).

### **Cell preparation**

Thymus, LN, and spleen were collected from 4 to 8-week old mice to obtain single cell suspensions by mechanical digestion. PBMCs were isolated from whole blood by using Histopaque-1083 reagent (Sigma Aldrich). The cells in the air pouch were collected as described above.

### **Spelenectomy and thymectomy**

The spleen was exposed by an oblique incision, in the left upper abdominal quadrant while the animal was kept under anesthesia with Avertin (2, 2, 2-Tribromoethanol) (Sigma Aldrich). After the splenic arteries and venous vessels were cauterized to minimize blood loss, the spleen was removed. The thymus was mechanically removed through an incision in the neck and thoracic wall extending to the level of the second rib, while mice were kept under anesthesia with Avertin. Sham-treated animals received identical manipulations without actual spleen and thymus removal prior to wound suturing.

### **DTH**

Mice were subcutaneously immunized with 200 µg of OVA protein in 200 µl of the emulsion consisting of an equal volume of PBS and complete Freund's adjuvant (CFA) (Sigma Aldrich). Ten days after the immunization, 100 µg of heat aggregated OVA in 50 µl of PBS was injected into the footpad. 24 h after the footpad injection, footpad thickness was measured and the intensity of inflammation was histologically evaluated.

### **Preparation of BM chimeric mice**

BM cells were obtained from DO11.10 and WT mice, and the resultant cells were mixed at the indicated ratio. After WT recipient mice were lethally irradiated (8 Gy), they received  $1 \times 10^7$  BM cells intravenously. The experiments were conducted on the obtained BM chimeric mice more than three weeks after transplantation.

### **In vivo transfection of tRANTES**

cDNA encoding mouse tRANTES (its nucleotide sequence described in Supporting Information Figure 6) was subcloned into the pLIVE expression plasmid vector (Mirus, Madison, WI). 10 µg of the resultant or empty pLIVE expression plasmid vector was injected into mice by using TransIT®-EE Delivery Solution (Mirus) according to the manufacturer's instructions, because this gene delivery system can sustain serum tRANTES levels at higher than 1 ng/ml for 2 months after the injection (our unpublished data).

### **Immunohistochemical analysis**

Mouse footpads were cut off and fixed in fixating agent, Yufix (Sakura Finetec Japan, Tokyo, Japan). After subsequent decalcification with formic acid (Nacalai Tesque, Kyoto, Japan), the samples were embedded with paraffin and sliced at 3 µm thickness. For Ag retrieval, the deparaffinized slides were autoclaved in 10 mmol/L citrate buffer (pH 6.0) for 10 min at 120 °C. After blocking with a protein block serum-free solution

(DAKO, Carpinteria, CA), anti-Foxp3 Ab (FJK-26s) was added to the tissue sections and incubated overnight in a humidified box at 4°C. Immune complexes were then detected using the CSA systems (DAKO) followed by staining with hematoxylin.

### **Determination of chemokine concentrations**

Concentrations of MCP-1/CCL2, TARC/CCL17, MDC/CCL22, RANTES/CCL5 and SDF-1/CXCL12 in the air pouch fluid were determined by Quantikine ELISA kit (R&D systems) according to the manufacturer's instructions.

### **FCM**

Single cell suspensions were stained with various combinations of fluorescent dye-conjugated or non-conjugated specific Abs in magnetic-activated cell sorting buffer (PBS supplemented with 2 mM EDTA and 3 % FBS). For non-conjugated Abs, fluorescence-conjugated secondary Abs were used. Subsequently, the cells were fixed, permeabilized and stained with a Foxp3 staining set (eBioscience). Subsequently, the expression of each molecule was analyzed using FACSCanto II (BD Biosciences) with the help of FlowJo (TreeStar, Ashland, OR).

### **Statistical analysis**

Data are represented as mean and SD. Statistical significance was determined by indicated method in each experiment. A value of  $p < 0.05$  was considered statistically significant.

### **Acknowledgements**

We would like to express our sincere appreciation to Dr. Joost J. Oppenheim (NCI-Frederick, Frederick, MD) for his critical comments on the manuscript. This work was supported by Grant-in-aid for scientific research in Japan (23790532). The funders had no role in study design, data collection and analysis, decision to publish,

or preparation of the manuscript.

**Conflict-of-Interest disclosures**

The authors declare no financial or commercial conflict of interest.

## References

- 1 **Shaw, C. M., Alvord, E. C., Jr., Fahlberg, W. J. and Kies, M. W.**, Adjuvant-antigen relationships in the production of experimental "allergic" encephalomyelitis in the guinea pig. *The Journal of experimental medicine* 1962. **115**: 169-179.
- 2 **Pabst, O. and Mowat, A. M.**, Oral tolerance to food protein. *Mucosal immunology* 2012. **5**: 232-239.
- 3 **Felton, L. D.**, The significance of antigen in animal tissues. *J. Immunol.* 1949. **61**: 107-117.
- 4 **Critchfield, J. M., Racke, M. K., Zuniga-Pflucker, J. C., Cannella, B., Raine, C. S., Goverman, J. and Lenardo, M. J.**, T cell deletion in high antigen dose therapy of autoimmune encephalomyelitis. *Science* 1994. **263**: 1139-1143.
- 5 **Liblau, R. S., Tisch, R., Shokat, K., Yang, X., Dumont, N., Goodnow, C. C. and McDevitt, H. O.**, Intravenous injection of soluble antigen induces thymic and peripheral T-cells apoptosis. *Proc. Natl. Acad. Sci. U. S. A.* 1996. **93**: 3031-3036.
- 6 **Aichele, P., Kyburz, D., Ohashi, P. S., Odermatt, B., Zinkernagel, R. M., Hengartner, H. and Pircher, H.**, Peptide-induced T-cell tolerance to prevent autoimmune diabetes in a transgenic mouse model. *Proc. Natl. Acad. Sci. U. S. A.* 1994. **91**: 444-448.
- 7 **Malek, T. R.**, The biology of interleukin-2. *Annu. Rev. Immunol.* 2008. **26**: 453-479.
- 8 **Webster, K. E., Walters, S., Kohler, R. E., Mrkvan, T., Boyman, O., Surh, C. D., Grey, S. T. and Sprent, J.**, In vivo expansion of T reg cells with IL-2-mAb complexes: induction of resistance to EAE and long-term acceptance of islet allografts without immunosuppression. *The Journal of experimental medicine* 2009. **206**: 751-760.
- 9 **Baba, T., Nakamoto, Y. and Mukaida, N.**, Crucial contribution of thymic Sirp alpha+ conventional dendritic cells to central tolerance against blood-borne antigens in a CCR2-dependent manner. *J. Immunol.* 2009. **183**: 3053-3063.
- 10 **Baba, T., Badr Mel, S., Tomaru, U., Ishizu, A. and Mukaida, N.**, Novel Process of

- Intrathymic Tumor-Immune Tolerance through CCR2-Mediated Recruitment of Sirpalpha(+) Dendritic Cells: A Murine Model. *PLoS One* 2012. **7**: e41154.
- 11 **Sallusto, F. and Baggiolini, M.**, Chemokines and leukocyte traffic. *Nature immunology* 2008. **9**: 949-952.
- 12 **Mukaida, N. and Baba, T.**, Chemokines in tumor development and progression. *Exp. Cell Res.* 2012. **318**: 95-102.
- 13 **Ingersoll, M. A., Platt, A. M., Potteaux, S. and Randolph, G. J.**, Monocyte trafficking in acute and chronic inflammation. *Trends in immunology* 2011. **32**: 470-477.
- 14 **Chen, D., Zhang, N., Fu, S., Schroppel, B., Guo, Q., Garin, A., Lira, S. A. and Bromberg, J. S.**, CD4+ CD25+ regulatory T-cells inhibit the islet innate immune response and promote islet engraftment. *Diabetes* 2006. **55**: 1011-1021.
- 15 **Wei, S., Kryczek, I. and Zou, W.**, Regulatory T-cell compartmentalization and trafficking. *Blood* 2006. **108**: 426-431.
- 16 **Yurchenko, E., Tritt, M., Hay, V., Shevach, E. M., Belkaid, Y. and Piccirillo, C. A.**, CCR5-dependent homing of naturally occurring CD4+ regulatory T cells to sites of *Leishmania major* infection favors pathogen persistence. *The Journal of experimental medicine* 2006. **203**: 2451-2460.
- 17 **Burstein, H. J. and Abbas, A. K.**, In vivo role of interleukin 4 in T cell tolerance induced by aqueous protein antigen. *The Journal of experimental medicine* 1993. **177**: 457-463.
- 18 **Thorstenson, K. M. and Khoruts, A.**, Generation of anergic and potentially immunoregulatory CD25+CD4 T cells in vivo after induction of peripheral tolerance with intravenous or oral antigen. *J. Immunol.* 2001. **167**: 188-195.
- 19 **Gottschalk, R. A., Corse, E. and Allison, J. P.**, Expression of Helios in peripherally induced Foxp3+ regulatory T cells. *J. Immunol.* 2012. **188**: 976-980.
- 20 **Akimova, T., Beier, U. H., Wang, L., Levine, M. H. and Hancock, W. W.**, Helios expression is a marker of T cell activation and proliferation. *PloS one* 2011. **6**:

- e24226.
- 21 **Bluestone, J. A. and Abbas, A. K.**, Natural versus adaptive regulatory T cells. *Nature reviews. Immunology* 2003. **3**: 253-257.
- 22 **Josefowicz, S. Z., Niec, R. E., Kim, H. Y., Treuting, P., Chinen, T., Zheng, Y., Umetsu, D. T. and Rudensky, A. Y.**, Extrathymically generated regulatory T cells control mucosal TH2 inflammation. *Nature* 2012. **482**: 395-399.
- 23 **Masteller, E. L., Tang, Q. and Bluestone, J. A.**, Antigen-specific regulatory T cells--ex vivo expansion and therapeutic potential. *Semin. Immunol.* 2006. **18**: 103-110.
- 24 **Tang, Q., Henriksen, K. J., Bi, M., Finger, E. B., Szot, G., Ye, J., Masteller, E. L. et al.**, In vitro-expanded antigen-specific regulatory T cells suppress autoimmune diabetes. *The Journal of experimental medicine* 2004. **199**: 1455-1465.
- 25 **Gardner, J. M., Fletcher, A. L., Anderson, M. S. and Turley, S. J.**, AIRE in the thymus and beyond. *Curr. Opin. Immunol.* 2009. **21**: 582-589.
- 26 **Scott-Browne, J. P., Shafiani, S., Tucker-Heard, G., Ishida-Tsubota, K., Fontenot, J. D., Rudensky, A. Y., Bevan, M. J. and Urdahl, K. B.**, Expansion and function of Foxp3-expressing T regulatory cells during tuberculosis. *The Journal of experimental medicine* 2007. **204**: 2159-2169.
- 27 **Belkaid, Y., Piccirillo, C. A., Mendez, S., Shevach, E. M. and Sacks, D. L.**, CD4+CD25+ regulatory T cells control *Leishmania* major persistence and immunity. *Nature* 2002. **420**: 502-507.
- 28 **Belkaid, Y.**, Role of Foxp3-positive regulatory T cells during infection. *Eur. J. Immunol.* 2008. **38**: 918-921.
- 29 **Curiel, T. J.**, Regulatory T cells and treatment of cancer. *Curr. Opin. Immunol.* 2008. **20**: 241-246.
- 30 **Yu, P., Gregg, R. K., Bell, J. J., Ellis, J. S., Divekar, R., Lee, H. H., Jain, R. et al.**, Specific T regulatory cells display broad suppressive functions against experimental allergic encephalomyelitis upon activation with cognate antigen. *J.*

- Immunol.* 2005. **174**: 6772-6780.
- 31 **Tarbell, K. V., Yamazaki, S., Olson, K., Toy, P. and Steinman, R. M.,** CD25+ CD4+ T cells, expanded with dendritic cells presenting a single autoantigenic peptide, suppress autoimmune diabetes. *The Journal of experimental medicine* 2004. **199**: 1467-1477.
- 32 **Beyer, M. and Schultze, J. L.,** Regulatory T cells in cancer. *Blood* 2006. **108**: 804-811.
- 33 **Sanchez, A. M. and Yang, Y.,** The role of natural regulatory T cells in infection. *Immunol. Res.* 2011. **49**: 124-134.
- 34 **Zhang, N., Schroppel, B., Lal, G., Jakubzick, C., Mao, X., Chen, D., Yin, N. et al.,** Regulatory T cells sequentially migrate from inflamed tissues to draining lymph nodes to suppress the alloimmune response. *Immunity* 2009. **30**: 458-469.
- 35 **Onizuka, S., Tawara, I., Shimizu, J., Sakaguchi, S., Fujita, T. and Nakayama, E.,** Tumor rejection by in vivo administration of anti-CD25 (interleukin-2 receptor alpha) monoclonal antibody. *Cancer Res.* 1999. **59**: 3128-3133.
- 36 **Bromley, S. K., Mempel, T. R. and Luster, A. D.,** Orchestrating the orchestrators: chemokines in control of T cell traffic. *Nature immunology* 2008. **9**: 970-980.
- 37 **Woodland, D. L. and Kohlmeier, J. E.,** Migration, maintenance and recall of memory T cells in peripheral tissues. *Nature reviews. Immunology* 2009. **9**: 153-161.
- 38 **Mora, J. R. and von Andrian, U. H.,** T-cell homing specificity and plasticity: new concepts and future challenges. *Trends in immunology* 2006. **27**: 235-243.
- 39 **Belkaid, Y. and Tarbell, K. V.,** Arming Treg cells at the inflammatory site. *Immunity* 2009. **30**: 322-323.
- 40 **Suffia, I., Reckling, S. K., Salay, G. and Belkaid, Y.,** A role for CD103 in the retention of CD4+CD25+ Treg and control of *Leishmania major* infection. *J. Immunol.* 2005. **174**: 5444-5455.
- 41 **Edwards, J. C., Sedgwick, A. D. and Willoughby, D. A.,** The formation of a structure

with the features of synovial lining by subcutaneous injection of air: an in vivo tissue culture system. *The Journal of pathology* 1981. **134**: 147-156.

## Legends to Figures

### **Figure 1. Preferential migration of Ag-specific Treg cells to the Ag-containing site**

(A) Schematic presentation of the experimental procedures of the air pouch model. (B) Infiltrating cells were collected from the air pouch at the indicated time points. After the cell numbers were determined, the cells were analyzed using FCM by gating on KJ1-26-high region. The absolute KJ1-26<sup>high</sup>Foxp3<sup>+</sup> cell numbers as Treg-cell numbers (left), the absolute KJ1-26<sup>high</sup>FoxP3<sup>-</sup> cell numbers as Teff-cell numbers (middle), and the proportion of Foxp3<sup>+</sup> and Foxp3<sup>-</sup> cells among KJ1-26<sup>high</sup> cells in the air pouch (right) are shown. Data are shown as mean +SD of 5 samples pooled from 2 experiments. \*\*  $p < 0.01$ , one-way ANOVA followed by Tukey-Kramer test. (C) DO11.10 mice were treated with the air pouch protocol and additionally, 100  $\mu$ g of OVA or BSA in 1 ml of PBS was injected into the air pouch. 24 h after the injection, the cells were obtained from the air pouch. Air pouch-infiltrating cells were analyzed by gating on KJ1-26-high region, and data are shown as mean + SD of 5 samples pooled from 2 independent experiments. \*  $p < 0.05$ , Student's t-test. (D) Lymphocytes were obtained from DO11.10 mice, which were immunized or non-immunized with the protocol shown in Supporting Information Figure 1A. The resultant cells were labeled with CFSE and were transferred into WT mice. Thereafter, 100  $\mu$ g of OVA in 1 ml of PBS was injected into the air pouch of WT mice. 72 h after the injection, the cells were obtained from air pouch or axillary LNs (dLN). The total cells in the air pouch and dLNs were analyzed on Foxp3 and CFSE by gating on KJ1-26-high region, and representative results from 3 independent experiments are shown.

### **Figure 2. Intravenous OVA injection-induced Treg-cell expansion in thymus**

(A) OVA was intravenously injected twice on Day 0 and Day 1 into DO11.10 mice. Thymus was collected on Day 0, Day 3 and Day 5. After the cell numbers were determined, the resultant thymocytes were analyzed for the expression of KJ1-26 and

Foxp3 by using FCM and the absolute numbers of KJ1-26<sup>high</sup>Foxp3<sup>+</sup> cells were calculated. The data are shown as mean + SD of 5 samples pooled from 2 independent experiments. \*\* $p < 0.01$ , one-way ANOVA followed by Tukey-Kramer test. (B) On Day 5, PBMCs were obtained from DO11.10 mice, which were immunized twice with OVA. The total resultant cells were analyzed for the expression of CD25 and Foxp3 after gating on KJ1-26 high region by using FCM. As a control, PBMCs were obtained from untreated DO11.10 mice. The percentage of CD25<sup>high</sup>Foxp3<sup>+</sup> or CD25<sup>low</sup>Foxp3<sup>+</sup> cells is shown in each panel. Representative results from 5 independent animals are shown. (C) Thymectomy, splenectomy or sham surgery was performed on DO11.10 mice. Two weeks after the operation, 2 mg of OVA was intravenously injected twice, on Day 0 and Day 1. On Day 3, PBMCs were collected and analyzed by FCM. The fold change in Treg cells is shown as mean + SD of 4 samples pooled from 2 experiments. \* $p < 0.05$ ; N.S., not significant, Student's t-test. (D) Total thymocytes or splenocytes collected on Day 0 or Day 3 were analyzed for Helios expression after gating on KJ1-26<sup>high</sup>Foxp3<sup>+</sup> cells. Data are shown as mean + SD of 4 animals pooled from 2 experiments. \* $p < 0.05$ ; \*\* $p < 0.01$ , one-way ANOVA followed by Tukey-Kramer test. (E) Helios expression on KJ1-26<sup>high</sup>Foxp3<sup>+</sup> cells (gray-filled histogram) or KJ1-26<sup>high</sup>Foxp3<sup>-</sup> cells (dashed-line histogram) from peripheral blood was analyzed by FCM, and representative results from 3 independent experiments are shown. The value shown indicates % positive cells among KJ1-26<sup>high</sup>Foxp3<sup>+</sup> cells. (F) Peripheral lymphocytes, which were obtained from DO11.10 mice un-immunized or immunized with OVA, were administered to WT mice with air pouches. 2 mg of OVA was intravenously injected twice only into WT mice, which received unimmunized, naïve lymphocytes. Finally, 100  $\mu$ g of OVA was further injected into the air pouch of WT mice receiving DO11.10 mouse-derived lymphocytes (Supporting Information Figure 1B). The total cells in the air pouch were obtained to determine the proportion of Foxp3<sup>+</sup> cells among KJ1-26<sup>high</sup> cells. Data are shown as mean + SD of 4 samples pooled from 3 independent experiments. \* $p < 0.05$ , Student's t-test.

**Figure 3. Ag-specific Treg-cell migration to the Ag-containing site in a CCR2- or CCR4-dependent manner**

(A) On Day 5 of the air pouch model, cells were obtained from the air pouch (gray-filled histograms) and the dLN (black line histograms) of DO11.10 mice. The cells were analyzed for the expression levels of chemokine receptors among KJ1-26<sup>high</sup>Foxp3<sup>+</sup> Treg cells (top) and KJ1-26<sup>high</sup>Foxp3<sup>-</sup> Teff cells (bottom). Values shown indicate % positive cells among air pouch-infiltrating cells. Representative data from 5 independent experiments are shown. (B) DO11.10 or DO11.10/CCR2<sup>-/-</sup> mice were treated as shown in Figure 1A. The total cells were obtained on Day 5 from the air pouch and dLNs. The ratios of Foxp3<sup>+</sup> cells among KJ1-26<sup>high</sup> cells (left), the absolute numbers of KJ1-26<sup>high</sup>Foxp3<sup>+</sup> cells from air pouch (middle) and the ratio of KJ1-26<sup>high</sup>Foxp3<sup>+</sup> cells from dLNs (right) were determined and shown as mean + SD of 5 individual animals pooled from 2 experiments. \*  $p < 0.05$ ; \*\*  $p < 0.01$ , Student's t-test. (C) Lymphocytes were obtained from DO11.10 mice or DO11.10/CCR2<sup>-/-</sup>, which were immunized as shown in Supporting Information Figure 1A. The resultant cells were labeled with CFSE and were transferred into WT mice. Thereafter, 100  $\mu$ g of OVA in 1 ml of PBS was injected into the air pouch of WT mice. 72 h after the injection, the cells were obtained from air pouch or dLNs. The total cells in the air pouch and dLNs were analyzed for Foxp3 by gating on KJ1-26<sup>high</sup> and CFSE-positive region, and representative results from 3 independent experiments are shown.

**Figure 4. Combined administration of OVA and IL-2 ICs suppresses OVA-induced inflammation.**

(A) Schematic presentation of induction procedures of Ag-specific DTH reactions. (B) BM chimeric mice with about 15 % lymphocytes expressing KJ1-26 (Supporting Information Figure 8) were treated as in Figure 4A. Skin tissues were obtained on Day 16 for histological evaluation using H&E staining. Representative results from 5

individual animals are shown; scale bar, 100  $\mu$ m. (C) Paw thickness was determined and the changes in thickness ( $\Delta$ mm) were calculated by subtracting the original thickness from the thickness of swollen paw. Data are shown as mean + SD of 5 animals from a single experiment performed. \*\*  $p < 0.01$ ; N.S., not significant, one-way ANOVA followed by Tukey-Kramer test. (D) BM chimeric mice were immunized twice with 2 mg of OVA. Peripheral blood was obtained on Day 10 to determine the proportion of CD25<sup>high</sup>KJ1-26<sup>high</sup>Foxp3<sup>+</sup> or CD25<sup>high</sup>V $\alpha$ 2<sup>+</sup>Foxp3<sup>+</sup> cells among lymphocytes, shown as mean  $\pm$  SD of 5 animals from an experiment. V $\alpha$ 2 TCR was used as a marker of polyclonal Treg cells. \*\*  $p < 0.01$ ; N.S., not significant, Student's t-test. (E) Skin tissues were obtained on Day 16. The tissues were stained with anti-Foxp3 Ab. The proportions of Foxp3<sup>+</sup> cells among mononuclear cells were determined by using Image J and shown as mean + S D of 5 individual animals from a single experiment performed. \*\*  $p < 0.01$ , one-way ANOVA followed by Tukey-Kramer test.

**Figure 5. Reversal of OVA and IL-2 ICs-induced suppression of DTH by blockade of CCR2.**

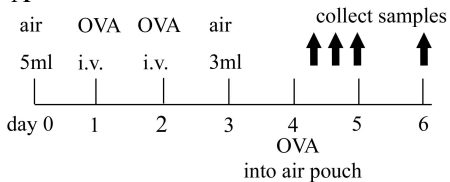
(A) DTH was elicited in BM chimeric mice, with 15% lymphocytes consisting of either DO11.10 or DO11.10/CCR2<sup>-/-</sup> lymphocytes. The tissues were obtained 1 day after OVA injection into the footpad and were processed to H&E staining. Representative results from 5 individual animals are shown; scale bar, 100  $\mu$ m. (B) The changes in thickness ( $\Delta$ mm) were determined when the tissues were obtained shown in Figure 5A. Data are shown as mean + SD of 5 individual animals from a single experiment performed. (C) The same tissues used in Figure 5B were stained with anti-Foxp3 Ab. The proportions of Foxp3<sup>+</sup> cells to mononuclear cells were determined by using Image J and shown as mean + SD of 5 individual animals from a single experiment performed. \*\*  $p < 0.01$ ; N.S., not significant, one-way ANOVA followed by Tukey-Kramer test.

**Figure 6. Combined IL-2 ICs and Ag treatment inhibits the DTH by efficient expansion of Ag-specific Treg cells.**

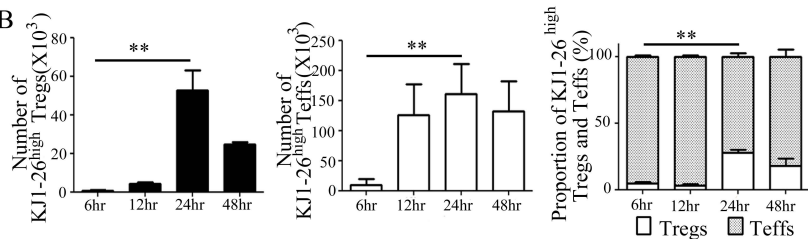
WT mice were treated intravenously with either IL-2 ICs, OVA alone or the combination of OVA and IL-2 ICs. Thereafter, DTH was elicited in WT mice as shown in Figure 4A. (A) Skin tissues were obtained on Day 16 and were stained with H&E for histological analysis. Representative results from 5 individual animals are shown; scale bar, 100  $\mu$ m. (B) Paw thickness on Day 16 was determined and shown as mean + SD were calculated of 5 individual from a single experiment performed. \*\*  $p < 0.01$ ; N.S., not significant, one-way ANOVA followed by Tukey-Kramer test.

Figure 1

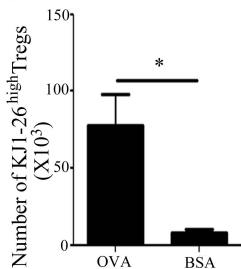
A



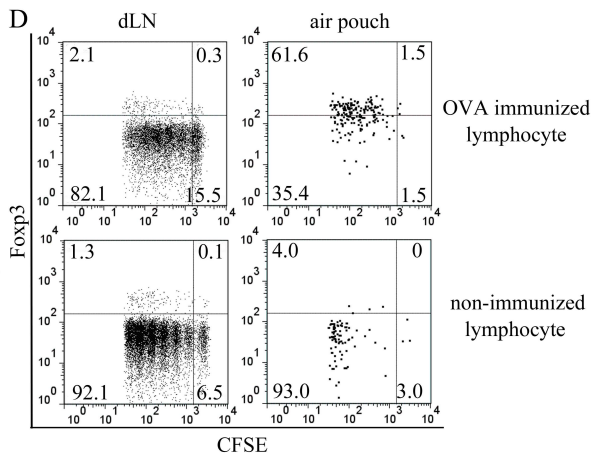
B



C



D



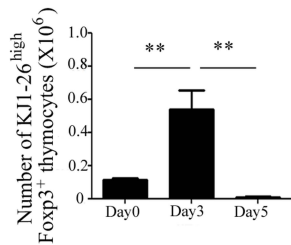
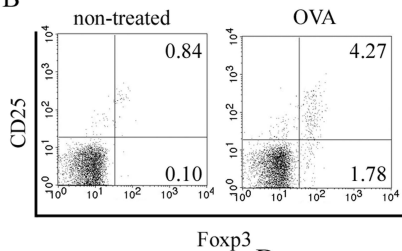
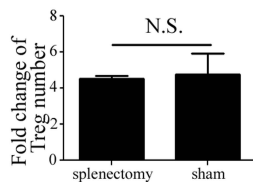
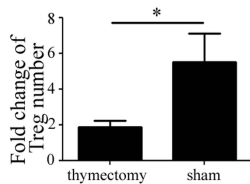
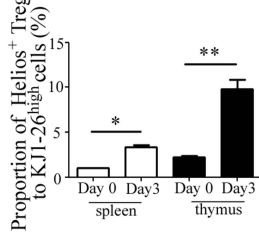
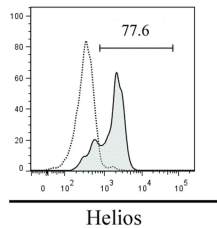
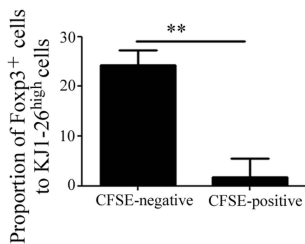
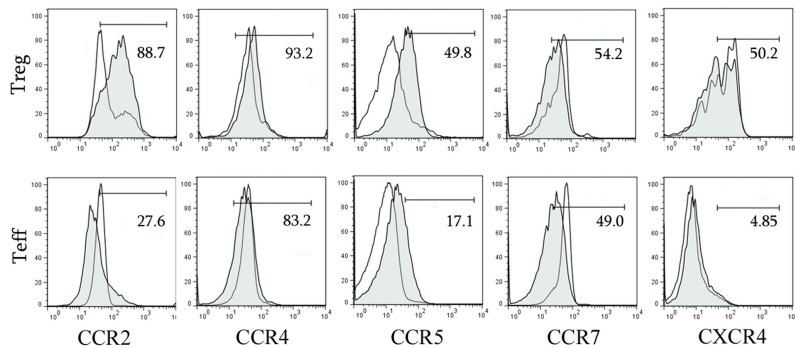
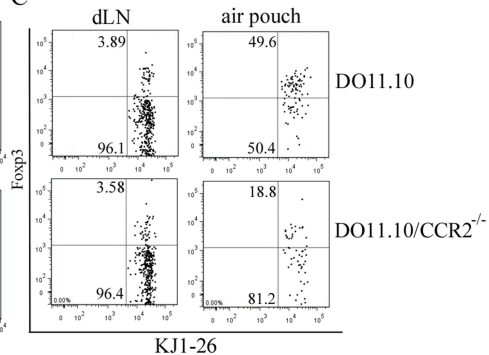
**Figure 2****A****B****C****D****E****F**

Figure 3

A



C



B

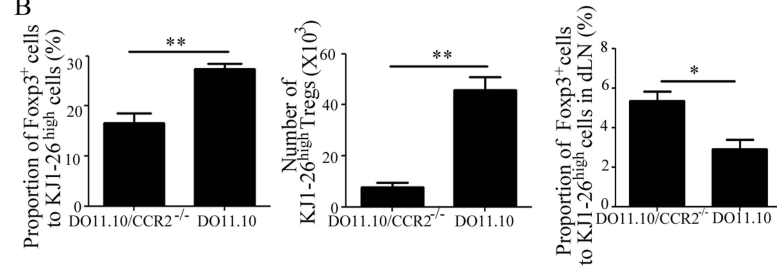
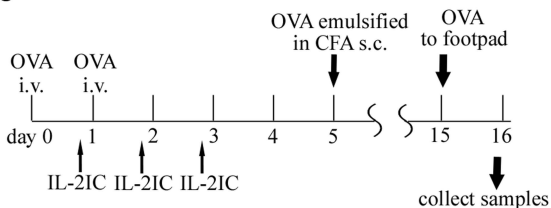
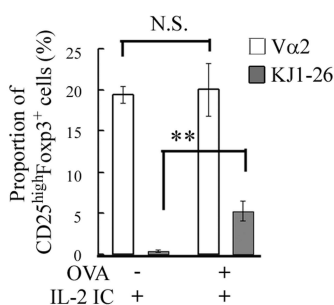


Figure 4

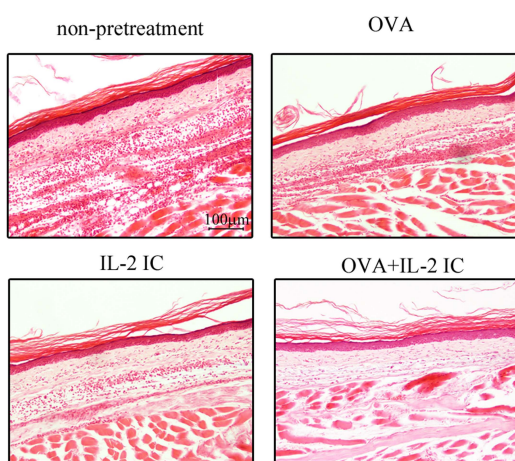
A



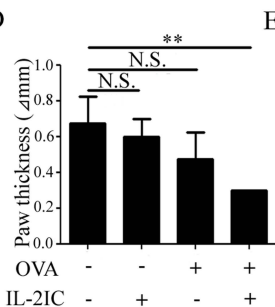
B



C



D



E

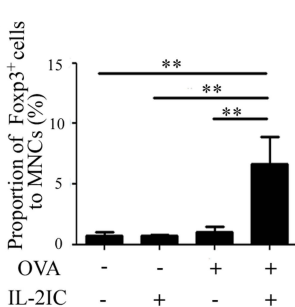
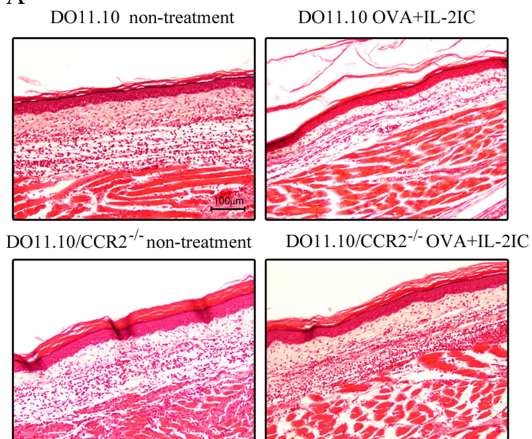
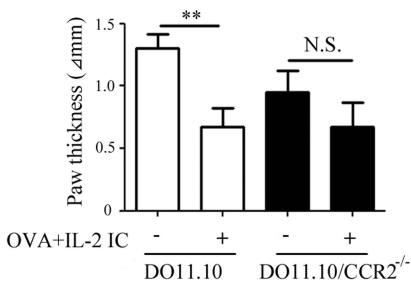


Figure 5

A



B



C

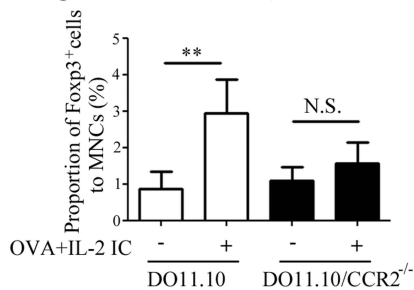
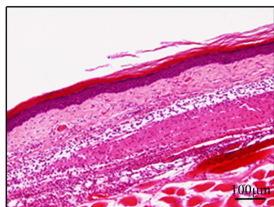
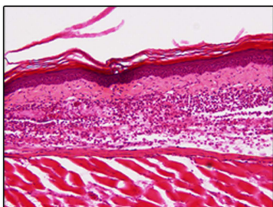


Figure 6

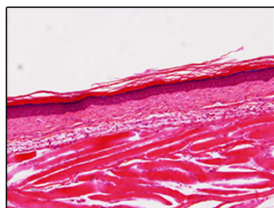
A



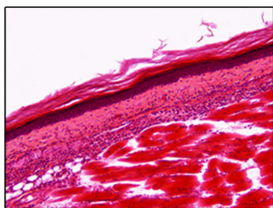
no-pretreatment



IL-2 IC

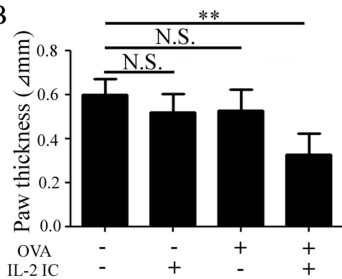


OVA



OVA+IL-2 IC

B



## **Legends to Supplemental Figures**

### **S1. Nucleotide sequence of tRANTES**

The inserted tRANTES nucleotide sequence is shown. Blue and red sequence encodes RANTES signal peptide and 9-68 RANTES (mature peptide), respectively.

### **S2. Gating strategy of Tregs and Teffs**

Cells were stained by KJ1-26 and Foxp3. The cells were gated on FSC/SSC for lymphocyte and further gated on KJ1-26<sup>high</sup>Foxp3<sup>+</sup> cells for Tregs and KJ1-26<sup>high</sup>Foxp3<sup>-</sup> cells for Teffs.

### **S3. Schematics presentation of adoptive transfer experiment**

(A) Lymphocytes were obtained from DO11.10 mice, which were untreated or injected twice with 2 mg of OVA. The obtained cells were labeled with CFSE and transferred to wild-type mice bearing the air pouch. Three days after OVA injection to air pouch, the cells were collected from the air pouch for the analysis with FCM. (B) Lymphocytes were obtained from DO11.10 and were transduced into another DO11.10 mouse after CFSE labeling. OVA was injected into air pouch with or without prior repeated intravenous OVA injection. Air pouch infiltrating cells were collected and analyzed by using FCM.

### **S4. Expression of Foxp3 and KJ1-26 in thymocytes after intravenous OVA injection**

OVA was intravenously injected twice on Day 0 and Day 1 into DO11.10 mice. Thymocytes were collected on Day 0 and Day 3 and were analyzed by using FCM. Numbers in quadrants indicate the percentage of cells in the designated gate. Representative results from 5 independent experiments are shown here.

### **S5. Alteration of KJ1-26<sup>high</sup>Foxp3<sup>-</sup> thymocytes after intravenous OVA injection**

OVA was intravenously injected twice on Day 0 and Day 1 into DO11.10 mice. Thymus was collected on Day 0 and Day 3. After the cell numbers were determined, the resultant thymocytes were analyzed for the expression of KJ1-26 and Foxp3 by using FCM and the absolute numbers of KJ1-26<sup>high</sup>Foxp3<sup>-</sup> cells were calculated. The mean and SD from 5 independent experiments are shown here. Student's t-test was used for statistical analysis. N.S., not significant.

### **S6. Alteration of chemokine expression in the air pouch after OVA injection**

DO11.10 mice were treated as shown in Figure 1A. The fluids in the air pouch were obtained at the indicated time intervals after OVA injection into the air pouch. The concentrations of CCL2, CCL5, CCL17, and CCL22 in the air pouch were determined on 5 individual animals by using ELISA. Mean and SD were calculated from 5 individual animals. Significant difference to control group are shown here. One-way ANOVA followed by Tukey-Kramer test was used for statistical analysis. \*,  $p < 0.05$ ; \*\*,  $p < 0.01$ .

### **S7. Effects of CCR4-signal blockade on the mobilization of OVA-specific Tregs**

DO11.10 mice were immunized twice with 2 mg of OVA on Day 1 and 2. On Day 4, 100 µg of anti-CCL17 or anti-CCL22 Ab was intravenously injected 1 hr before OVA injection into the air pouch (Figure 1A). As a control, rat control IgG was injected. The cells were obtained on Day 5 from the air pouch and the draining lymph node to determine the proportion of KJ1-26<sup>high</sup>Foxp3<sup>+</sup> cells. Proportion of Foxp3<sup>+</sup> cells to KJ1-26<sup>high</sup> cells (left), the number of KJ1-26<sup>high</sup>Foxp3<sup>+</sup> cells from air pouch (middle) and the proportion of Foxp3<sup>+</sup> cells to KJ1-26<sup>high</sup> cells in draining lymph node (right) are shown. Mean and SD were calculated from 5 individual animals and are shown here. One-way ANOVA followed by Tukey-Kramer test was used for statistical analysis. \*,  $p < 0.05$ ; \*\*,  $p < 0.01$ ; N.S., not significant.

**S8. Effects of CCR5-signal blockade on the mobilization of OVA-specific Tregs**

Ten  $\mu\text{g}$  of pLIVE-tRANTES vector was *in vivo* transfected 5 days before air pouch formation. As a control, control pLIVE vector was transfected. DO11.10 mice were immunized twice with 2 mg of OVA on Day 0 and Day 1. OVA was injected into the air pouch on Day 4 (Figure 1A). The cells were obtained on Day 5 from air pouch and the draining lymph node to determine the proportion of KJ1-26<sup>high</sup>Foxp3<sup>+</sup> cells. Proportion of Foxp3<sup>+</sup> cells to KJ1-26<sup>high</sup> cells (left), the number of KJ1-26<sup>high</sup>Foxp3<sup>+</sup> cells from air pouch (middle) and the proportion of Foxp3<sup>+</sup> cells to KJ1-26<sup>high</sup> cells in the draining lymph node (right) are shown. Mean and SD were calculated from 3 individual animals and are shown here. Student's t-test was used for statistical analysis. N.S., not significant.

**S9. Chimerism of DO11.10 TCR expressing T cells in BM chimera**

Peripheral blood was obtained from BM chimera to determine the proportion of KJ1-26<sup>high</sup> cells to CD4<sup>+</sup> cells. Percentage of CD4<sup>+</sup>KJ1-26<sup>high</sup> and CD4<sup>+</sup>KJ1-26<sup>negative to low</sup> cells are shown.

**S10. Expansion of polyclonal Tregs by IL-2 IC treatment**

BM chimeric mice were daily injected with IL-2 IC for 3 days. Three days after the last IL-2 IC injection, expression of CD25 and Foxp3 on V $\alpha$ 2<sup>+</sup> (upper panels) and KJ1-26<sup>high</sup> cells (lower panels) were observed. Percentage of CD25<sup>high</sup>Foxp3<sup>+</sup> and CD25<sup>low</sup>Foxp3<sup>+</sup> cells are shown in each panel.

**S11. Effects of CCR4 blockade on antigen-induced immune reaction in DTH**

BM chimeric mice were treated with the protocol shown in Figure 4A. Anti-CCL17 was intravenously injected 1 hr before OVA injection to footpad. As a control, rat-IgG was injected. Paw thickness were determined on 5 individual animals. The changes in thickness ( $\Delta\text{mm}$ ) were calculated by subtracting the original thickness from the

thickness of swollen paw. Mean and SD were calculated from 5 individual animals and are shown here. One-way ANOVA followed by Tukey-Kramer test was used for statistical analysis. \*,  $p < 0.05$ ; \*\*,  $p < 0.01$ ; N.S., not significant.

Figure S1

Insert: Signal peptide (RANTES signal peptide) + 9-68 RANTES (mature peptide)

GTCGACATGAAGATCTCTGCAGCTGCCCTCACCATCATCTCACTGCAGCCGCCCTCTGCACCCCCGCA  
 Sal I  
 CCTGCCGAATTCCTCTGCTTTGCCTACCTCTCCCTCGCGTGCCTCGTGCCACGTCAAGGAGTAT  
 EcoRI  
 TTCTACACCAGCAGCAAGTGTCCAATCTTGCAGTCGTGTTTGTCACTCGAAGGAACCGCCAAGTGTGT  
 GCCAACCCAGAGAAGAAGTGGGTTCAAGAATACATCAACTATTTGGAGATGAGCGGATCCCGGGCTGA  
 TTACAAGGACGACGATGATGACAAGTAGGGATCC  
 FLAG sequence BamHI

Figure S2

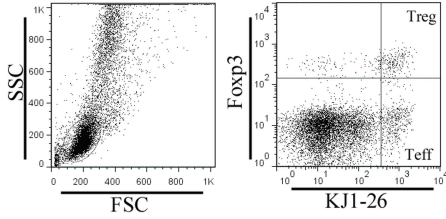


Figure S3

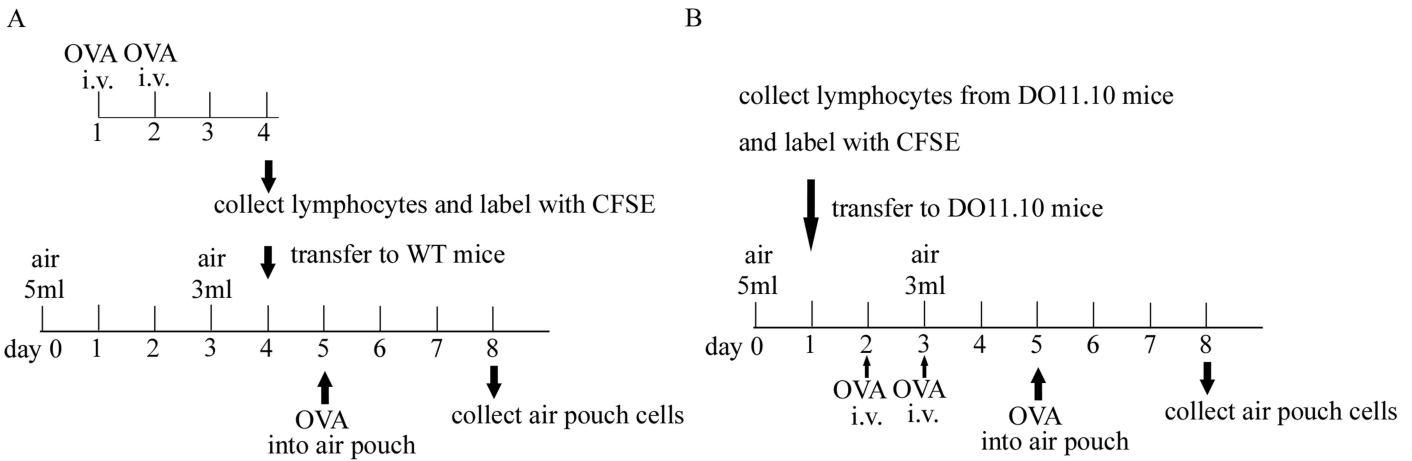


Figure S4

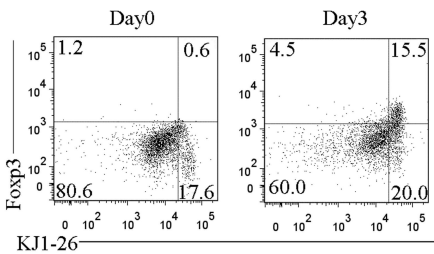


Figure S5

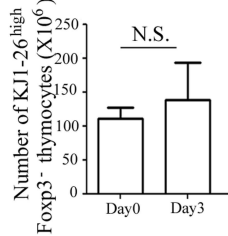


Figure S6

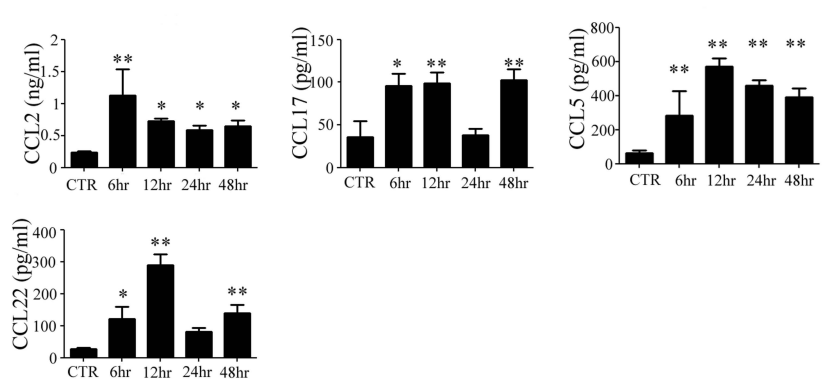


Figure S7

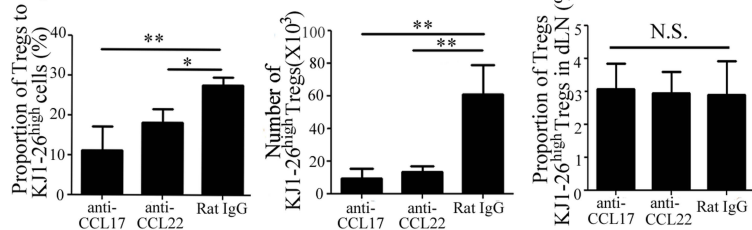


Figure S8

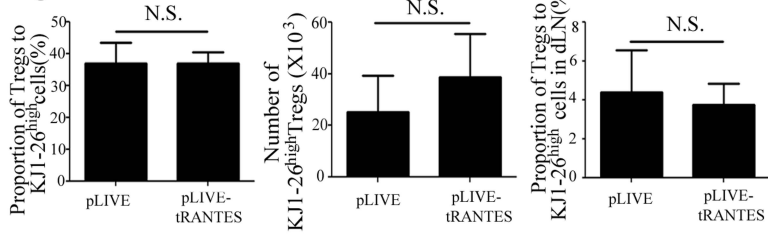


Figure S9

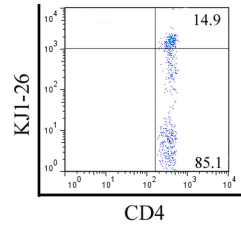


Figure S10

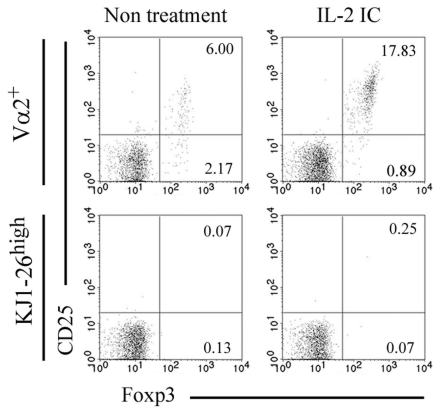


Figure S11

